PHOTONICS Research

# Control of soft X-ray high harmonic spectrum by using two-color laser pulses

Cheng Jin[1,*] and C. D. Lin[2]

[1]Department of Applied Physics, Nanjing University of Science and Technology, Nanjing 210094, China
[2]J. R. Macdonald Laboratory, Department of Physics, Kansas State University, Manhattan, Kansas 66506, USA
*Corresponding author: cjin@njust.edu.cn

Received 1 February 2018; revised 28 February 2018; accepted 1 March 2018; posted 5 March 2018 (Doc. ID 321155); published 23 April 2018

**We demonstrate the suppression of soft X-ray high harmonics generated by two-color laser pulses interacting with Ne gas in a gas cell. We show that harmonic suppression can occur at the proper combination of the propagation distance and gas pressure. The physical mechanism behind is the phase mismatch between "short"-trajectory harmonics generated at the early and later times through the interplay of geometric phase, dispersion, and plasma effects. In addition, we demonstrate that the position and depth of harmonic suppression can be tuned by increasing the gas pressure. Furthermore, the suppression can be extended to other laser focusing configurations by properly scaling macroscopic parameters. Our investigation reveals a simple and novel experimental scheme purely relying on the phase mismatch for selectively controlling soft X-ray tabletop light sources without adopting the filters for applications.** 

***OCIS codes:*** (190.2620) Harmonic generation and mixing; (190.7110) Ultrafast nonlinear optics; (340.7480) X-rays, soft x-rays, extreme ultraviolet (EUV); (320.7120) Ultrafast phenomena.

https://doi.org/10.1364/PRJ.6.000434

## 1. INTRODUCTION

High-order harmonic generation (HHG) is a nonlinear up-conversion process resulting from the interaction of an intense focused infrared laser pulse with a gaseous target. It offers a unique coherent tabletop light source ranging from the extreme ultraviolet (XUV) to X-rays with femtosecond or attosecond durations [1–3]. Due to its exceptional coherence property in space and time, it has been employed extensively in many ultrafast experiments, such as in attosecond science [4], nanoscale structure imaging [5], assisted free-electron lasers [6], and HHG spectroscopy [7]. In some applications, for instance, for multi-spectral spectrometry [8], element-specific coherent imaging [9], and photoionization/emission experiments employing soft X-ray HHG sources [10], it is desirable to control the spectral structure of the generated HHG spectrum. It is generally understood that HHG is very sensitive to the properties of the driving lasers and the gas medium, and the spectral distribution can be varied either by modifying the single-atom response or by changing the macroscopic phase-matching conditions [11,12].

The manipulation of harmonic spectrum has been achieved in a variety of approaches, for example, by adaptive pulse shaping of the driving laser [13], multi-color waveform synthesis [14], and quasi-phase matching (QPM) [15,16]. Early works from the Kapteyn–Murnane group [17,18] demonstrated that the efficiency of the desired XUV discrete harmonics can be enhanced by an order of magnitude by pulse shaping. Between 2013 and 2014, Wei *et al.* [19,20] showed experimentally that a single harmonic among the harmonic comb can be greatly enhanced by controlling the sub-cycle waveform by synthesizing the fundamental laser and its second and third harmonic fields with perpendicular polarizations. Recently, Lerner *et al.* [21] proposed, through numerical simulation, that selected harmonics can be significantly suppressed by adding one or two phase-mismatched segments. In the mean time, high harmonics can also be suppressed by taking advantage of the electronic structure of atoms or molecules. According to the quantitative rescattering (QRS) model [22], single-atom harmonic spectrum can be written as the product of a returning electron wave packet and the photo-recombination cross-section (PRCS). Thus the "minimum" structure in the PRCS would lead to suppression of harmonics in the single-atom spectrum. Such minimum could be preserved after macroscopic propagation in a gaseous medium under certain conditions [23]. A well-known example is the "Cooper minimum" in Ar observed in high harmonic spectra [24–30]. Other examples include the minimum in PRCS due to multi-electron effects, which appears in the measured HHG spectrum of Xe [31]. For

molecules, similar minimum in the harmonic spectra has been observed in aligned $N_2$ molecules [32–36] and $CO_2$ molecules [37–40], and even for unaligned polyatomic molecules [41]. However, the suppression of high harmonics by solely making use of macroscopic phase-matching conditions has not been systematically explored.

In recent years, it has become possible to control optical waveform of the driving lasers by synthesizing multi-color laser pulses [42–45] to optimize the yields of high harmonics (see the review [46]). In our recent works we have focused on the optimization of multi-color laser waveform for the enhancement of harmonic yields [47], the improvement of two-color harmonic divergence in soft X-rays [48,49], as well as the macroscopic scaling of HHG generated by a two-color laser in a hollow waveguide [50]. In this article, we address whether the optimized multi-color waveform can be employed to control the spectral structure of HHG by adjusting macroscopic phase-matching conditions.

The main goal of this paper is to propose a scheme to selectively suppress soft X-ray high harmonics by using two-color optimized waveform with proper macroscopic conditions. We will then demonstrate the phase-mismatch mechanism leading to the suppression of harmonics in such spectral regions. The article is arranged as follows: in Section 2, we will show the HHG spectra of two-color optimized laser pulses versus gas pressure in a given configuration. In Section 3, we will show the conditions for the suppression to occur and uncover the phase-mismatch mechanism by analyzing the evolution of harmonic spectra, electric fields, and temporal behavior of harmonic emissions along the propagation direction at different gas pressures. We will show that harmonic suppression can be tuned by varying the gas pressure. In Section 4, the scaling of harmonic divergence and yields will be given under different phase-matching conditions. The conclusion of this article is given in Section 5.

## 2. HARMONICS GENERATED IN A GAS CELL BY AN OPTIMIZED TWO-COLOR WAVEFORM

A complete description of an HHG process includes the interaction between a single atom and the driving laser pulse, and the macroscopic propagation of the fundamental and the harmonic fields in a gaseous medium [51–53]. This amounts to solving the coupled time-dependent Schrödinger equation (TDSE) and the three-dimensional Maxwell wave equation (MWE) [54]. In the present simulation, we choose Ne as the target distributed uniformly inside the gas cell. Instead of solving the TDSE, the harmonics from each individual atom are calculated by the QRS model [22].

The two-color optimized waveform obtained in Ref. [47] is applied to realistic pulses written as

$$E(t) = E_1 A_1(t)\cos(\omega_1 t + \phi_1) + E_2 A_2(t)\cos(\omega_2 t + \phi_2). \quad (1)$$

Here $E_i$, $\omega_i$, $A_i$, and $\phi_i$ $(i = 1, 2)$ are the respective amplitude, angular frequency, envelope, and phase of each pulse. Laser parameters adopted in this work are listed in Table 1. Note that pulse durations of the two colors are different.

**Table 1. Laser Parameters for a Two-Color Laser Pulse[a]**

| $\lvert E_1\rvert^2$ | $\lvert E_2\rvert^2$ | $\phi_1$ | $\phi_2$ | FWHM1 | FWHM2 |
|---|---|---|---|---|---|
| 1.98 | 1.32 | 0 | $1.36\pi$ | 21.3 | 10.7 |

[a]Laser intensities for the two colors ($|E_1|^2$ and $|E_2|^2$) are in units of $10^{14}$ W/cm$^2$. $\lambda_1$ is 1600 nm, and $\lambda_2 = \lambda_1/3$. Full width at half-maximum (FWHM) durations of the temporal envelopes [$A_1(t)$ and $A_2(t)$] are in units of femtoseconds.

We first check if the two-color laser pulse could keep the characteristics of the optimized waveform in Ref. [47]. Figure 1(a) shows the simulated single-atom harmonic spectra using a two- and a single-color laser pulses, respectively. To maintain the same cutoff energy, the single-color 1.6-μm laser was chosen with the peak intensity of $3.0 \times 10^{14}$ W/cm$^2$ and the full width at half-maximum (FWHM) duration of 21.3 fs. We can see that the two-color pulse can enhance harmonic yield by about one to two orders of magnitude over the one-color pulse. Time-frequency analysis of the harmonic emission driven by the two-color pulse is displayed in Fig. 1(b). It shows that "short"-trajectory electron emissions dominate over "long"-trajectory electron ones (harmonic emissions from multiple returns are artificially removed in the simulation). Thus the optimized waveform is expected to generate harmonics that are favorable for phase matching in the macroscopic propagation.

We next examine the harmonic spectra generated in a 2-mm-long gas cell whose center is placed 2 mm after the laser focus in order to efficiently select harmonics emitted by "short"-trajectory electrons. To ensure that the two colors have the same Rayleigh length, the beam waists of the 1.6- and 0.533-μm lasers are chosen to be 40 and 23.1 μm, respectively. By varying other laser parameters, we manage to preserve the two-color waveform in Table 1 at the center of the gas cell only when the gas pressure is very low. In Fig. 1(c), the harmonic spectra at the exit plane of the gas cell for various gas pressures from 10 to 400 Torr are shown. (The spectra are smoothed by using Bezier curve for easy comparison.) The best balance between the largest harmonic yields in the plateau region and the highest cutoff energy can be achieved when the gas pressure is increased to 200 Torr. This is considered to be the optimal pressure in the given configuration. Beyond it, the harmonic yields are gradually reduced by further increasing gas pressure. At 400 Torr, the harmonics around 120 eV are seen to be greatly suppressed, leading to a pronounced "minimum". This minimum is not associated with the minimum in the PRCS of the target since no such minimum exists in Ne [55]. In-depth discussion of the harmonic suppression will be further conducted later.

In Fig. 1(d), we show the harmonic emission in the far field at the optimal pressure of 200 Torr. It can be seen that harmonics covering from 70 to 250 eV are well localized along the propagation axis and their divergence is less than 2 mrad, indicating that good phase matching has been achieved. The behavior of harmonics obtained from the optimized two-color laser pulses in a gas cell is very similar to those generated in a hollow waveguide [48,49].

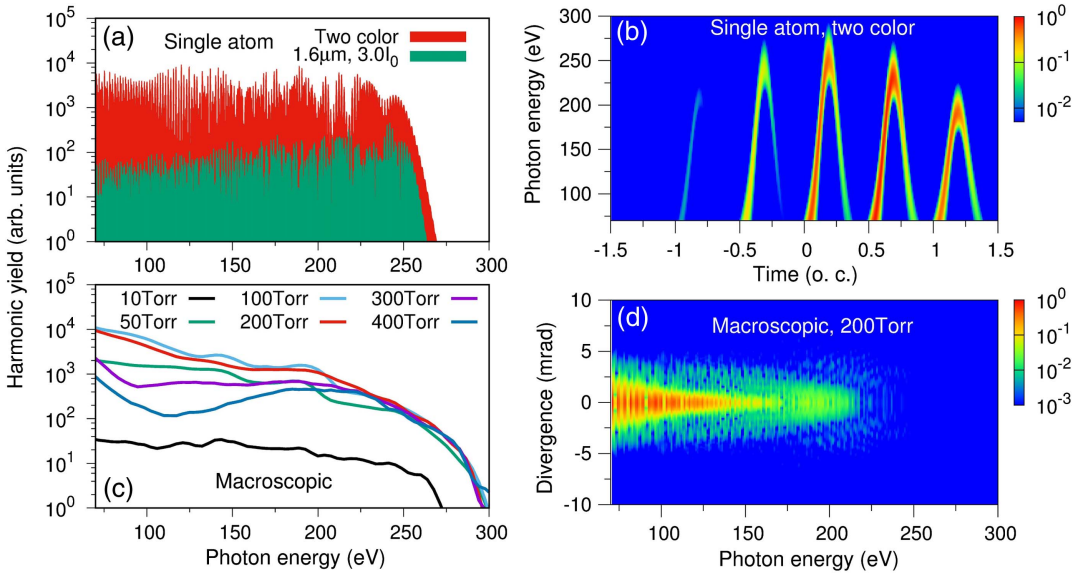


**Fig. 1.** (a) Single-atom harmonic yields with a 1.6-μm and a two-color laser pulse. The corresponding time-frequency harmonic emissions by the two-color pulse are shown in (b). (c) Macroscopic harmonic spectra (integrated over the exit plane of the gas cell and smoothed by using Bezier curve) generated by the two-color laser pulse at different gas pressures. Optimal pressure for the highest harmonic yields and the largest cutoff energy was found to be 200 Torr. The angular divergence of the far-field harmonic generated at this pressure is shown in (d). See text for other laser parameters.

## 3. SUPPRESSION OF SOFT X-RAY HARMONICS GENERATED BY A TWO-COLOR LASER PULSE

### A. Dependence of the HHG Suppression on Macroscopic Parameters and Optical Effects

To reveal the physical mechanism of the harmonic suppression in Fig. 1(c) at 400 Torr, we investigate the influence of parameters that are known to affect the generation of harmonics; for example, the propagation distance (or length of gas cell), the dispersion and absorption of harmonics by the gas medium, and the gas pressure.

In Fig. 2(a), we show how the suppression of high harmonics around 120 eV evolves with the propagation distance for the gas pressure at 400 Torr in a 2-mm-long gas cell. The suppression is not significant until the propagation distance reaches

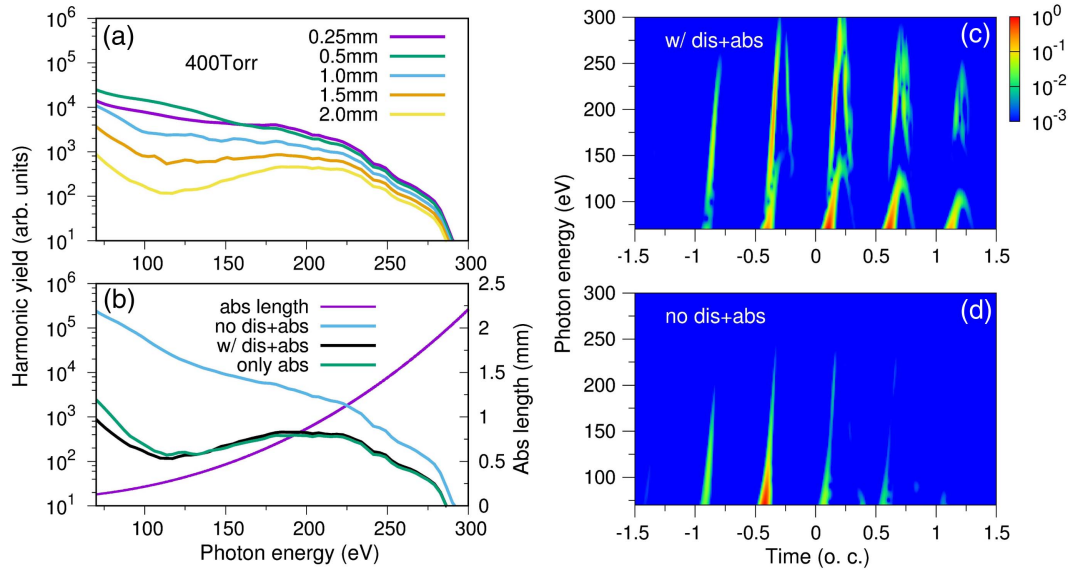


**Fig. 2.** (a) Evolution of harmonic spectra against the propagation distance by a two-color laser pulse at the gas pressure of 400 Torr. The propagation distances are as indicated. (b) The harmonic spectrum at the exit of the gas cell calculated including both dispersion and absorption effects (w/dis + abs) is compared with calculations where only absorption (only abs) is included, and with calculations where neither absorption nor dispersion (no dis + abs) is included. The absorption length versus harmonic energy for gas pressure at 400 Torr from NIST [56] is also plotted (see right-hand scale). (c), (d) Time-frequency analysis of the harmonic emissions (normalized) at $r = 11$ μm of the exit plane. The optical cycle (o.c.) is defined with respect to the fundamental 1.6-μm laser.

1.5 mm. From the absorption length plotted in Fig. 2(b), this is about 4 to 5 times longer than the absorption length. In Fig. 2(b), the effects of dispersion and absorption of harmonics by the gas medium are analyzed for harmonics at the exit plane. Without both (blue curve), the simulated harmonics, especially the lower-energy ones, are clearly much stronger than the harmonics calculated including both effects (black curve). Comparing to calculations that include only absorption (green curve), it is clear that strong absorption near the 120 eV region is the major factor responsible for the appearance of the minimum in the harmonic spectra.

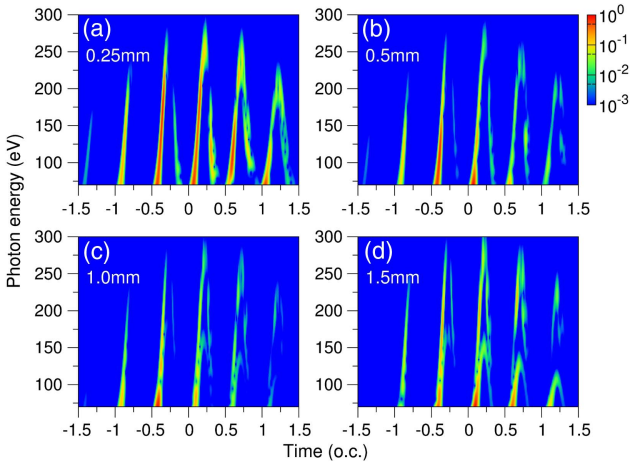


**Fig. 3.** Time-frequency analysis of the harmonic emissions (normalized) at $r = 11$ μm at different propagation planes for the gas pressure of 400 Torr including both dispersion and absorption effects. The optical cycle (o.c.) is defined with respect to the fundamental 1.6-μm laser.

Further insight into the suppression can be obtained by time-frequency analysis of the harmonic emission at the exit plane, as shown in Figs. 2(c) and 2(d) for cases with and without including dispersion and absorption effects, respectively. With the inclusion of both, for the time interval between −0.5 and 1.0 optical cycle, there are low-energy harmonics with the cutoff energy at about 150 eV and strong "short"-trajectory high-energy harmonics within each major emission in each half optical cycle. This is actually the result of the interference of all harmonics generated from the propagation distance $d = 0$ to 2 mm. The evolution of harmonic emissions with the propagation distance in Fig. 3 indicates that the harmonics generated in the first (or second) half of the gas cell mostly contribute to the harmonic emission with the higher (or lower) cutoff energy. Due to the likely phase mismatch between the two groups of harmonics, their interferences finally cause the harmonic minimum appearing at around 120 eV. We will further uncover its origin in the next section. When the dispersion and absorption are excluded in the simulation, only one harmonic burst from "short"-trajectory electrons appears in each half optical cycle, see Fig. 2(d). Thus there is no suppression in the simulated spectra near 120 eV.

Does the suppression of harmonics occur only for relatively large propagation distance or only for high gas pressure? To answer this question, we choose two pressures: 50 and 200 Torr, and study similar HHG spectra dependence of the propagation distance in Figs. 4(a) and 4(b), and time-frequency analysis of harmonic emissions in Figs. 4(c) and 4(d). For both pressures, suppression of the harmonics is not found at any propagation distances considered, and there is only one harmonic burst from "short"-trajectory emission in each half optical cycle. This shows that suppression of harmonics could occur at an appropriate combination of the propagation distance and gas pressure, for example, at propagation distance of 1.5 or 2 mm and gas pressure of 400 Torr.

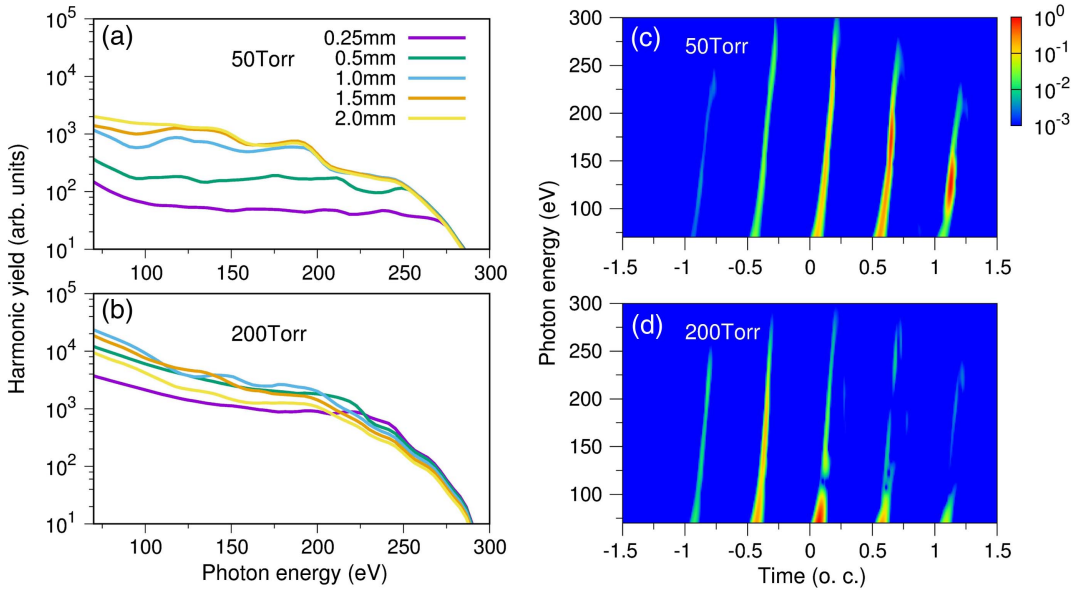


**Fig. 4.** Evolution of macroscopic two-color harmonic spectra with the propagation distance (as indicated) for two gas pressures: (a) 50 Torr and (b) 200 Torr. (c), (d) Time-frequency analysis of macroscopic harmonic emissions (normalized) at $r = 11$ μm of the exit plane.

### B. Analysis of the Origin of Harmonic Suppression by Delineating the Emission Time and the Time-Dependent Field of the Driving Laser

To understand the origin of the temporal emissions in Fig. 2(c) and Figs. 4(c) and 4(d), respectively, for three gas pressures of 400, 50, and 200 Torr, we inspect the temporal behavior of the electric field of the two-color laser in the reference frame (moving at the speed of light) at three propagation distances, $d = 0$, 1.0, and 2.0 mm, as shown in Fig. 5 for the field at an off-axis distance of $r = 11$ μm. Compared to the field at the entrance, we first note that the field is always reduced as it propagates in the medium. At 50 Torr, because of the geometric phase of the focused laser, the field is shifted to the left, see Fig. 5(a). As the pressure is increased, dispersion becomes significant, which can compensate for the geometric phase or even overtake it, leading to the shift of the electric field to the right, as shown by enlarged figures of the electric fields around −0.3 optical cycle on the leading edge in Figs. 5(b) and 5(c). This accounts for the emission of harmonics at the leading edge of the laser pulse. On the trailing edge, plasma defocusing plays a role to oppose the dispersion. That is why the propagated electric fields have shifted remarkably compared to initial ones, for instance, as shown by enlarged figures of the electric fields around 0.7 optical cycle in Figs. 5(b) and 5(c).

In Figs. 6(a)–6(c), time-frequency analysis of high harmonics caused by the propagated laser pulse in the middle ($d = 1$ mm) (already plotted in Fig. 5) of the gas cell is shown for three pressures. Harmonic emissions with considerable "short"-trajectory contributions are presented. The harmonic cutoff energies are seen to decrease with the increase of gas pressure. We line out the harmonic emissions at 120 eV (as indicated by the orange line) for the three pressures, and plot them together in Fig. 6(d). It clearly shows that the peak of the "short"-trajectory emission shifts to the right as gas pressure is increased. We plot the same pictures for $d = 1.5$ and 2 mm, in Figs. 6(e) and 6(f), respectively. With the increase of propagation distance, the peak of the "short"-trajectory emission shifts more to the right. Meanwhile, earlier generated high harmonics in the first half of the gas cell have the higher cutoff energies, and propagate faster close to the speed of light (appearing earlier in the reference frame than the harmonic bursts in Fig. 6). The temporal shift between earlier and newly generated "short"-trajectory harmonic emissions in the second half of the gas cell would lead to the substantial interference (or phase mismatch).

In short, here are the two main results: (i) the propagated laser pulse maintains the characteristics of the optimized waveform of Table 1 with strong "short"-trajectory harmonic emissions; (ii) the temporal shift of newly generated harmonic emissions in the reference frame depends on both propagation distance and gas pressure and the electric fields have been greatly reduced. These two factors explain why the harmonic suppression appears at low photon energies at the proper propagation distance and gas pressure in Fig. 1(c).

### C. Dependence of Harmonic Suppression on Gas Pressure: Two-Color versus One-Color Driving Lasers

Can the position and depth of the harmonic suppression observed at 400 Torr be tuned with the gas pressure? The HHG spectra at the exit plane of the 2-mm-long gas cell for different pressures calculated are shown in Fig. 7(a). By increasing the gas pressure from 400 to 800 Torr, the position of harmonic suppression gradually moves from 120 to 150 eV, and the

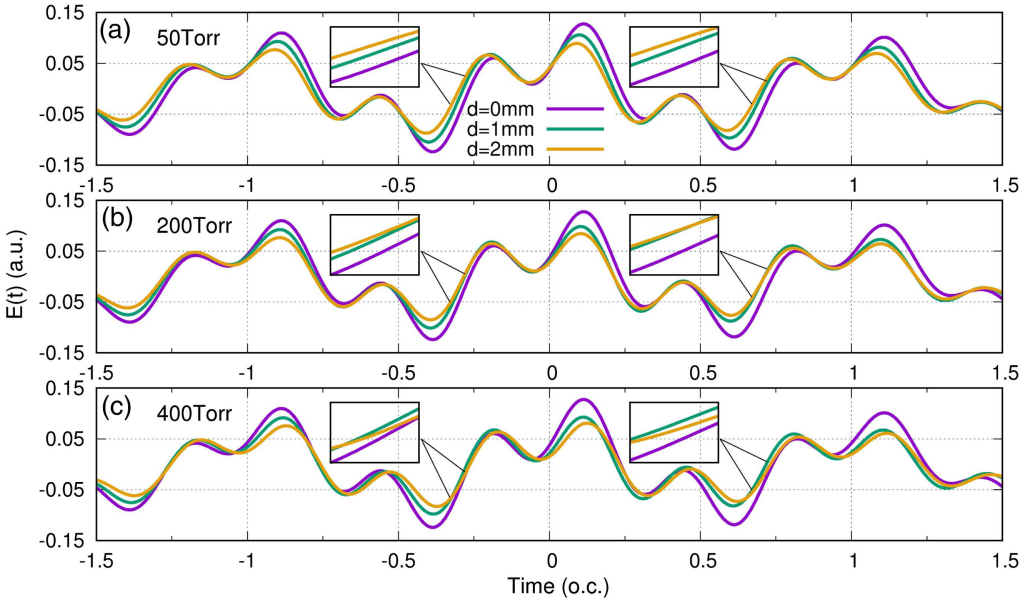


**Fig. 5.** Time-dependent electric fields of the two-color laser pulse at $r = 11$ μm for three gas pressures (a) 50 Torr, (b) 200 Torr, and (c) 400 Torr at three positions: $d = 0$ mm (at the entrance), $d = 1$ mm (in the middle), and $d = 2$ mm (at the exit plane of the gas cell), respectively. Enlarged figures of the electric fields are shown for the two time intervals, one at the leading edge and the other at the trailing edge of the pulse. Note that the driving field has been substantially weakened due to the geometric phase, the dispersion, and the plasma dispersion as the beam travels in space and time in the gas cell.

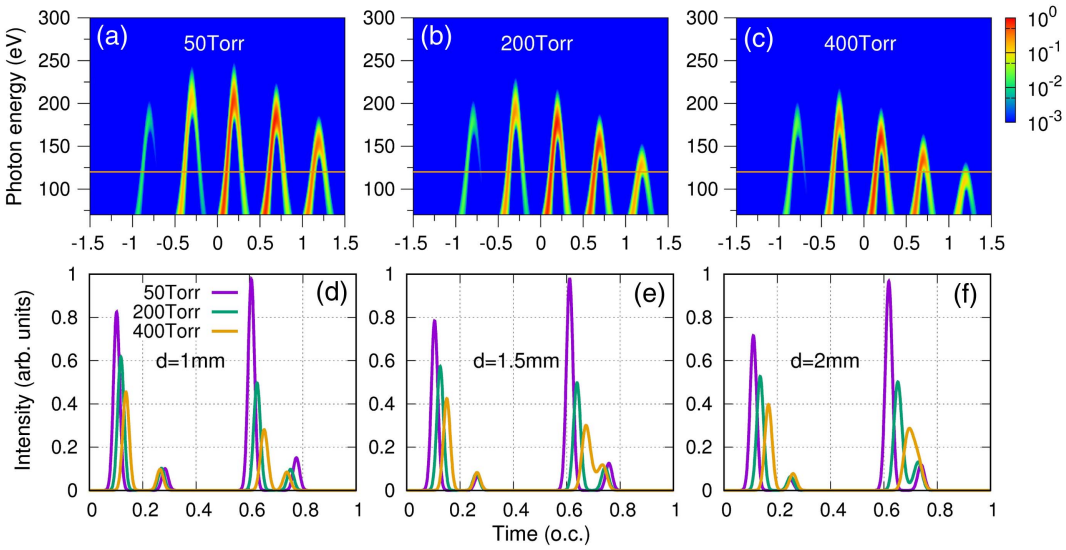


**Fig. 6.** Time-frequency analysis of harmonic emission driven by the electric field at $d = 1$ mm for an off-axis position, $r = 11$ μm (shown in Fig. 5) for three gas pressures: (a) 50 Torr, (b) 200 Torr, and (c) 400 Torr. The 120 eV harmonic emissions are lined out from (a)–(c) and replotted in (d) for the three pressures at $d = 1$ mm. The same plots are shown at (e) $d = 1.5$ mm and (f) $d = 2$ mm. One observes that each harmonic burst of "short"-trajectory electron emission changes in time depending on the gas pressure as well as the propagation distance.

growth of the suppression depth is monotonic. Note that the higher-energy harmonics are not modified by the increase of the gas pressure. Thus increasing the gas pressure has the effect of selecting only the higher harmonics without the need of a filter for removing the lower harmonics.

Can the suppression be carried out with one-color laser pulses? We simulated the harmonics with a 1.6-μm laser which has a beam waist of 40 μm at gas pressure from 200 to 800 Torr. The results are displayed in Fig. 7(b). The harmonic yields in the plateau gradually decrease with the pressure while

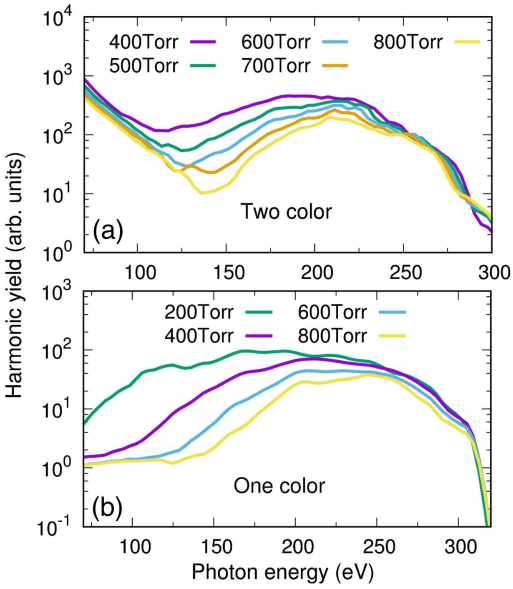


**Fig. 7.** Macroscopic harmonic spectra (smoothed by using Bezier curve for easy comparison) generated by (a) two-color and (b) 1.6-μm laser pulses at different gas pressures.

harmonics above 200 eV in the cutoff region do not change much. The harmonic suppression appears if we compare HHG spectrum of high pressure with that of low pressure. However, no clear minimum is visible due to the less efficient lower-order harmonics in the single-atom response [see Fig. 1(a)]. Thus one advantage of using two-color laser pulses is to create an apparent minimum in the HHG spectrum. Comparing the cutoff harmonics, the yields from the optimized two-color pulse are about one order of magnitude higher than the single-color one. This is another advantage of using optimized two-color laser pulses for selecting strong higher harmonics for applications.

## 4. MACROSCOPIC SCALING OF THE DIVERGENCE AND YIELD OF HARMONICS IN A GAS CELL

In the discussions above, we fixed the arrangement of driving laser and the gas cell. Can harmonic suppression take place in other configurations? To answer this question, we first need to properly scale the macroscopic parameters. Recently, a general scaling rule has been proposed [57–60] to keep the characteristics of the HHG process invariant for one-color lasers with the scaling

$$\begin{aligned} z &\to \eta^2 z, \\ w &\to \eta w, \\ l &\to \eta^2 l, \\ p &\to p/\eta^2. \end{aligned} \tag{2}$$

Here $\eta$ is a scaling parameter, $z$ is the longitudinal position in the reference frame, $w$ is the laser beam waist, $l$ is the length of the interaction medium, and $p$ is the gas pressure. We extend this scaling relation to two-color laser pulses. The macroscopic

**Table 2. Macroscopic Parameters for Harmonic Emissions in Fig. 8[a]**

| | $w_1$ (μm) | $w_2$ (μm) | $z_0$ (mm) | $l$ (mm) | $p$ (Torr) |
|---|---|---|---|---|---|
| (a) | 20.0 | 11.55 | 0.25 | 0.5 | 800.0 |
| (b) | 40.0 | 23.1 | 1.0 | 2.0 | 200.0 |
| (c) | 80.0 | 46.2 | 4.0 | 8.0 | 50.0 |
| (d) | 20.0 | 11.55 | 0.25 | 0.5 | 1600.0 |
| (e) | 40.0 | 23.1 | 1.0 | 2.0 | 400.0 |
| (f) | 80.0 | 46.2 | 4.0 | 8.0 | 100.0 |

[a] $w_1$ and $w_2$ are the beam waists of the 1.6- and 0.533-μm lasers, respectively. $z_0$ is the entrance position of gas cell respect to laser focus, $l$ is the length of gas cell, and $p$ is the gas pressure.

parameters for a more tightly or loosely focused configuration are listed in Table 2, together with that applied in the previous simulations. The harmonic emissions in the far field for two cases are shown in Fig. 8: the generation of optimal harmonics and the generation of suppressed harmonics. We can see that for both cases the harmonic emission patterns are identical, showing that harmonic divergence satisfies the following relation:

$$\mathrm{Div}(\omega) \to \mathrm{Div}(\omega)/\eta. \tag{3}$$

The total harmonic yields integrated over the radial distance are shown in Fig. 9. For both the optimal and suppressed harmonics, the shape of the harmonic spectra obtained from three arrangements looks the same, and the harmonic yields have been checked to fulfill the relation

$$S(\omega) \to \eta^2 S(\omega). \tag{4}$$

Two important points can be concluded from these simulations: (i) the scaling relation derived for one color laser in a gas cell can be extended to two-color laser pulses, and harmonic divergence can also be properly scaled, similar to harmonics generated in a hollow waveguide studied earlier [48]; (ii) harmonic suppression can be reproduced under other arrangements by properly scaling macroscopic parameters.

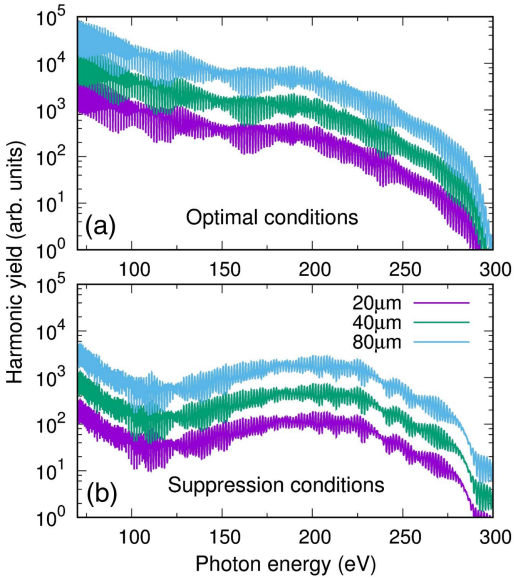


**Fig. 9.** Total harmonic yields integrated over the radial dimension under the (a) optimal and (b) suppression conditions. Panels (a) and (b) correspond to harmonic emissions in Figs. 8(a)–8(c) and in Figs. 8(d)–8(f), respectively. In both (a) and (b), the ratio of the harmonic yield between top, middle, and bottom curve is 16:4:1.

## 5. CONCLUSIONS

In summary, we studied the possibility of selectively controlling soft X-ray harmonics by using a two-color optimized laser pulse interacting with Ne gas in a gas cell. We first searched for the optimal conditions for two-color laser pulses to obtain the highest harmonic yields and cutoff energy, and well-localized harmonic emissions in the far field. We found that soft X-ray harmonics around 120 eV could be suppressed if gas pressure was increased to 400 Torr far beyond the optimal one at about 200 Torr, and the length of the gas cell was long enough

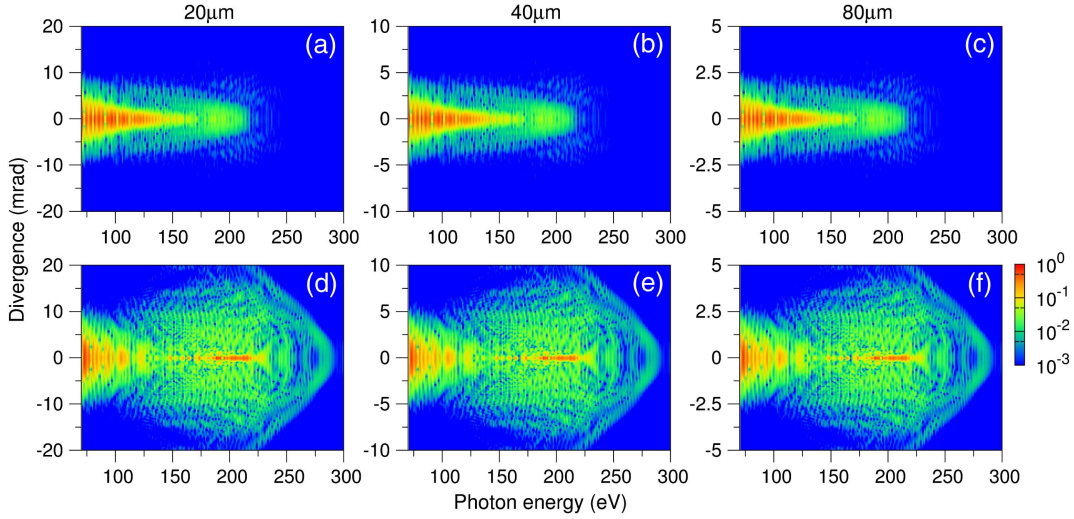


**Fig. 8.** Harmonic emission (normalized at the highest peak in each figure) in the far field using the optimized two-color laser pulses. (a)–(c) are for the generation of optimal harmonics, and (d)–(f) are for the generation of suppressed harmonics. The beam waists of the 1.6-μm laser in the two-color waveforms are indicated on top of the figures. Other parameters for (a)–(f) are listed in Table 2.

compared to the absorption length. The unique temporal harmonic emissions showed that interference between the major burst and a small one inside of it in each optical cycle was responsible for the harmonic suppression. We then analyzed the evolution of electric fields and new harmonic emissions along the propagation direction at different pressures, which revealed that the sufficient temporal shift of newly generated harmonic emissions (in the reference frame) depends on both the propagation distance and gas pressure. We further showed that the position and depth of the suppression could be tuned by increasing gas pressure. Finally, we showed that harmonic suppression can be found in other configurations by properly scaling macroscopic parameters.

Our study paves an easy and efficient route for suppressing soft X-ray harmonics without the need of employing proper filters. The scheme is scalable to longer driving laser wavelengths. We expect this work to stimulate further interest in studying macroscopic propagation effects for controlling high harmonics either within phase-matched or phase-mismatched spectral region in other free geometries, guided geometries, and beam truncated geometries [61–63] by using single- or multicolor laser pulses [64].

**Funding.** Fundamental Research Funds for the Central Universities of China (30916011207); National Natural Science Foundation of China (NSFC) (11774175); U.S. Department of Energy (DOE) (DE-FG02-86ER13491); Air Force Office of Scientific Research (AFOSR) (FA9550-14-1-0255).

**Acknowledgment.** C. Jin was supported by Fundamental Research Funds for the Central Universities of China and by NSFC. C. D. Lin was supported by Chemical Sciences, Geosciences and Biosciences Division, Office of Basic Energy Sciences, Office of Science, DOE, and by AFOSR.

## REFERENCES

1. F. Calegari, G. Sansone, S. Stagira, C. Vozzi, and M. Nisoli, "Advances in attosecond science," J. Phys. B **49**, 062001 (2016).
2. T. Popmintchev, M.-C. Chen, D. Popmintchev, P. Arpin, S. Brown, S. Alisauskas, G. Andriukaitis, T. Balciunas, O. D. Mücke, A. Pugzlys, A. Baltuska, B. Shim, S. E. Schrauth, A. Gaeta, C. Hernndez-Garcia, L. Plaja, A. Becker, A. Jaron-Becker, M. M. Murnane, and H. C. Kapteyn, "Bright coherent ultrahigh harmonics in the keV X-ray regime from mid-infrared femtosecond lasers," Science **336**, 1287–1291 (2012).
3. L.-Y. Peng, W.-C. Jiang, J.-W. Geng, W.-H. Xiong, and Q. Gong, "Tracing and controlling electronic dynamics in atoms and molecules by attosecond pulses," Phys. Rep. **575**, 1–71 (2015).
4. F. Krausz and M. Ivanov, "Attosecond physics," Rev. Mod. Phys. **81**, 163–234 (2009).
5. J. Miao, T. Ishikawa, I. K. Robinson, and M. M. Murnane, "Beyond crystallography: diffractive imaging using coherent X-ray light sources," Science **348**, 530–535 (2015).
6. G. Lambert, T. Hara, D. Garzella, T. Tanikawa, M. Labat, B. Carre, H. Kitamura, T. Shintake, M. Bougeard, S. Inoue, Y. Tanaka, P. Salieres, H. Merdji, O. Chubar, O. Gobert, K. Tahara, and M.-E. Couprie, "Injection of harmonics generated in gas in a free-electron laser providing intense and coherent extreme-ultraviolet light," Nat. Phys. **4**, 296–300 (2008).
7. Y. Pertot, C. Schmidt, M. Matthews, A. Chauvet, M. Huppert, V. Svoboda, A. von Conta, A. Tehlar, D. Baykusheva, J.-P. Wolf, and H. J. Wörner, "Time-resolved X-ray absorption spectroscopy with a water window high-harmonic source," Science **355**, 264–267 (2017).
8. A. Ozawa, J. Rauschenberger, C. Gohle, M. Herrmann, D. R. Walker, V. Pervak, A. Fernandez, R. Graf, A. Apolonski, R. Holzwarth, F. Krausz, T. W. Hänsch, and T. Udem, "High harmonic frequency combs for high resolution spectroscopy," Phys. Rev. Lett. **100**, 253901 (2008).
9. B. Zhang, D. F. Gardner, M. H. Seaberg, E. R. Shanblatt, C. L. Porter, R. Karl, C. A. Mancuso, H. C. Kapteyn, M. M. Murnane, and D. E. Adams, "Ptychographic hyperspectral spectromicroscopy with an extreme ultraviolet high harmonic comb," Opt. Express **24**, 18745–18754 (2016).
10. S. L. Cousin, N. Di Palo, B. Buades, S. M. Teichmann, M. Reduzzi, M. Devetta, A. Kheifets, G. Sansone, and J. Biegert, "Attosecond streaking in the water window: a new regime of attosecond pulse characterization," Phys. Rev. X **7**, 041030 (2017).
11. V. Tosa, H. T. Kim, I. J. Kim, and C. H. Nam, "High-order harmonic generation by chirped and self-guided femtosecond laser pulses. I. Spatial and spectral analysis," Phys. Rev. A **71**, 063807 (2005).
12. F. Wang, L. He, C. Zhai, W. Shi, Q. Zhang, P. Lan, and P. Lu, "Time-dependent phase matching of high-order-harmonic generation," Phys. Rev. A **92**, 063839 (2015).
13. C. Winterfeldt, C. Spielmann, and G. Gerber, "Colloquium: optimal control of high-harmonic generation," Rev. Mod. Phys. **80**, 117–140 (2008).
14. I. J. Kim, C. M. Kim, H. T. Kim, G. H. Lee, Y. S. Lee, J. Y. Park, D. J. Cho, and C. H. Nam, "Highly efficient high-harmonic generation in an orthogonally polarized two-color laser field," Phys. Rev. Lett. **94**, 243901 (2005).
15. X. Zhang, A. L. Lytle, T. Popmintchev, X. Zhou, H. C. Kapteyn, M. M. Murnane, and O. Cohen, "Quasi-phase-matching and quantum-path control of high-harmonic generation using counterpropagating light," Nat. Phys. **3**, 270–275 (2007).
16. A. Paul, R. A. Bartels, R. Tobey, H. Green, S. Weiman, I. P. Christov, M. M. Murnane, H. C. Kapteyn, and S. Backus, "Quasi-phase-matched generation of coherent extreme-ultraviolet light," Nature **421**, 51–54 (2003).
17. R. Bartels, S. Backus, E. Zeek, L. Misoguti, G. Vdovin, I. P. Christov, M. M. Murnane, and H. C. Kapteyn, "Shaped-pulse optimization of coherent emission of high-harmonic soft X-rays," Nature **406**, 164–166 (2000).
18. R. Bartels, S. Backus, I. P. Christov, H. C. Kapteyn, and M. M. Murnane, "Attosecond time-scale feedback control of coherent X-ray generation," Chem. Phys. **267**, 277–289 (2001).
19. P. Wei, J. Miao, Z. Zeng, C. Li, X. Ge, R. Li, and Z. Xu, "Selective enhancement of a single harmonic emission in a driving laser field with subcycle waveform control," Phys. Rev. Lett. **110**, 233903 (2013).
20. P. Wei, Z. Zeng, J. Jiang, J. Miao, Y. Zheng, X. Ge, C. Li, and R. Li, "Selective generation of an intense single harmonic from a long gas cell with loosely focusing optics based on a three-color laser field," Appl. Phys. Lett. **104**, 151101 (2014).
21. G. Lerner, T. Diskon, O. Neufeld, O. Kfir, and O. Cohen, "Selective suppression of high-order harmonics within phase-matched spectral regions," Opt. Lett. **42**, 1349–1352 (2017).
22. A. T. Le, R. R. Lucchese, S. Tonzani, T. Morishita, and C. D. Lin, "Quantitative rescattering theory for high-order harmonic generation from molecules," Phys. Rev. A **80**, 013401 (2009).
23. G. Wang, C. Jin, A.-T. Le, and C. D. Lin, "Conditions for extracting photoionization cross sections from laser-induced high-order-harmonic spectra," Phys. Rev. A **86**, 015401 (2012).
24. S. Minemoto, T. Umegaki, Y. Oguchi, T. Morishita, A. T. Le, S. Watanabe, and H. Sakai, "Retrieving photorecombination cross sections of atoms from high-order harmonic spectra," Phys. Rev. A **78**, 061402 (2008).
25. E. J. Takahashi, T. Kanai, Y. Nabekawa, and K. Midorikawa, "10 mJ class femtosecond optical parametric amplifier for generating soft X-ray harmonics," Appl. Phys. Lett. **93**, 041111 (2008).
26. P. Colosimo, G. Doumy, C. I. Blaga, J. Wheeler, C. Hauri, F. Catoire, J. Tate, R. Chirla, A. M. March, G. G. Paulus, H. G. Muller, P. Agostini, and L. F. DiMauro, "Scaling strong-field interactions towards the classical limit," Nat. Phys. **4**, 386–389 (2008).

27. H. J. Wörner, H. Niikura, J. B. Bertrand, P. B. Corkum, and D. M. Villeneuve, "Observation of electronic structure minima in high-harmonic generation," Phys. Rev. Lett. **102**, 103901 (2009).
28. C. Jin, H. J. Wörner, V. Tosa, A. T. Le, J. B. Bertrand, R. R. Lucchese, P. B. Corkum, D. M. Villeneuve, and C. D. Lin, "Separation of target structure and medium propagation effects in high-harmonic generation," J. Phys. B **44**, 095601 (2011).
29. J. P. Farrell, L. S. Spector, B. K. McFarland, P. H. Bucksbaum, M. Gühr, M. B. Gaarde, and K. J. Schafer, "Influence of phase matching on the Cooper minimum in Ar high-order harmonic spectra," Phys. Rev. A **83**, 023420 (2011).
30. J. Higuet, H. Ruf, N. Thiré, R. Cireasa, E. Constant, E. Cormier, D. Descamps, E. Mével, S. Petit, B. Pons, Y. Mairesse, and B. Fabre, "High-order harmonic spectroscopy of the Cooper minimum in argon: experimental and theoretical study," Phys. Rev. A **83**, 053401 (2011).
31. A. D. Shiner, B. E. Schmidt, C. Trallero-Herrero, H. J. Wörner, S. Patchkovskii, P. B. Corkum, J.-C. Kieffer, F. Légaré, and D. M. Villeneuve, "Probing collective multi-electron dynamics in xenon with high-harmonic spectroscopy," Nat. Phys. **7**, 464–467 (2011).
32. S. Haessler, J. Caillat, W. Boutu, C. Giovanetti-Teixeira, T. Ruchon, T. Auguste, Z. Diveki, P. Breger, A. Maquet, B. Carré, R. Taeb, and P. Salières, "Attosecond imaging of molecular electronic wavepackets," Nat. Phys. **6**, 200–206 (2010).
33. J. B. Bertrand, H. J. Wörner, P. Hockett, D. M. Villeneuve, and P. B. Corkum, "Revealing the Cooper minimum of $N_2$ by molecular frame high-harmonic spectroscopy," Phys. Rev. Lett. **109**, 143001 (2012).
34. C. Jin, J. B. Bertrand, R. R. Lucchese, H. J. Wörner, P. B. Corkum, D. M. Villeneuve, A.-T. Le, and C. D. Lin, "Intensity dependence of multiple orbital contributions and shape resonance in high-order harmonic generation of aligned $N_2$ molecules," Phys. Rev. A **85**, 013405 (2012).
35. X. Ren, V. Makhija, A.-T. Le, J. Troß, S. Mondal, C. Jin, V. Kumarappan, and C. Trallero-Herrero, "Measuring the angle-dependent photoionization cross section of nitrogen using high-harmonic generation," Phys. Rev. A **88**, 043421 (2013).
36. Y. Huang, C. Meng, X. Wang, Z. Lü, D. Zhang, W. Chen, J. Zhao, J. Yuan, and Z. Zhao, "Joint measurements of terahertz wave generation and high-harmonic generation from aligned nitrogen molecules reveal angle-resolved molecular structures," Phys. Rev. Lett. **115**, 123002 (2015).
37. O. Smirnova, Y. Mairesse, S. Patchkovskii, N. Dudovich, D. Villeneuve, P. Corkum, and M. Y. Ivanov, "High harmonic interferometry of multi-electron dynamics in molecules," Nature **460**, 972–977 (2009).
38. C. Vozzi, F. Calegari, E. Benedetti, J.-P. Caumes, G. Sansone, S. Stagira, M. Nisoli, R. Torres, E. Heesel, N. Kajumba, J. P. Marangos, C. Altucci, and R. Velotta, "Controlling two-center interference in molecular high harmonic generation," Phys. Rev. Lett. **95**, 153902 (2005).
39. R. Torres, T. Siegel, L. Brugnera, I. Procino, J. G. Underwood, C. Altucci, R. Velotta, E. Springate, C. Froud, I. C. E. Turcu, S. Patchkovskii, M. Y. Ivanov, O. Smirnova, and J. P. Marangos, "Revealing molecular structure and dynamics through high-order harmonic generation driven by mid-IR fields," Phys. Rev. A **81**, 051802 (2010).
40. C. Vozzi, M. Negro, F. Calegari, G. Sansone, M. Nisoli, S. De Silvestri, and S. Stagira, "Generalized molecular orbital tomography," Nat. Phys. **7**, 822–826 (2011).
41. M. C. H. Wong, A.-T. Le, A. F. Alharbi, A. E. Boguslavskiy, R. R. Lucchese, J.-P. Brichta, C. D. Lin, and V. R. Bhardwaj, "High harmonic spectroscopy of the Cooper minimum in molecules," Phys. Rev. Lett. **110**, 033006 (2013).
42. A. Wirth, M. T. Hassan, I. Grguraš, J. Gagnon, A. Moulet, T. T. Luu, S. Pabst, R. Santra, Z. A. Alahmed, A. M. Azzeer, V. S. Yakovlev, V. Pervak, F. Krausz, and E. Goulielmakis, "Synthesized light transients," Science **334**, 195–200 (2011).
43. S.-W. Huang, G. Cirmi, J. Moses, K.-H. Hong, S. Bhardwaj, J. R. Birge, L.-J. Chen, E. Li, B. J. Eggleton, G. Cerullo, and F. X. Kärtner, "High-energy pulse synthesis with sub-cycle waveform control for strong-field physics," Nat. Photonics **5**, 475–479 (2011).
44. E. J. Takahashi, P. Lan, O. D. Mücke, Y. Nabekawa, and K. Midorikawa, "Attosecond nonlinear optics using gigawatt-scale isolated attosecond pulses," Nat. Commun. **4**, 2691 (2013).
45. S. Haessler, T. Balčiunas, G. Fan, G. Andriukaitis, A. Pugžlys, A. Baltuška, T. Witting, R. Squibb, A. Zar, J. W. G. Tisch, J. P. Marangos, and L. E. Chipperfield, "Optimization of quantum trajectories driven by strong-field waveforms," Phys. Rev. X **4**, 021028 (2014).
46. C. Jin and C. D. Lin, "Optimization of multi-color laser waveform for high-order harmonic generation," Chin. Phys. B **25**, 094213 (2016).
47. C. Jin, G. Wang, H. Wei, A. T. Le, and C. D. Lin, "Waveforms for optimal sub-keV high-order harmonics with synthesized two- or three-colour laser fields," Nat. Commun. **5**, 4003 (2014).
48. C. Jin, G. J. Stein, K.-H. Hong, and C. D. Lin, "Generation of bright, spatially coherent soft X-ray high harmonics in a hollow waveguide using two-color synthesized laser pulses," Phys. Rev. Lett. **115**, 043901 (2015).
49. C. Jin, K.-H. Hong, and C. D. Lin, "Optimal generation of spatially coherent soft X-ray isolated attosecond pulses in a gas-filled waveguide using two-color synthesized laser pulses," Sci. Rep. **6**, 38165 (2016).
50. C. Jin, K.-H. Hong, and C. D. Lin, "Macroscopic scaling of high-order harmonics generated by two-color optimized waveforms in a hollow waveguide," Phys. Rev. A **96**, 013422 (2017).
51. E. Priori, G. Cerullo, M. Nisoli, S. Stagira, S. De Silvestri, P. Villoresi, L. Poletto, P. Ceccherini, C. Altucci, R. Bruzzese, and C. de Lisio, "Nonadiabatic three-dimensional model of high-order harmonic generation in the few-optical-cycle regime," Phys. Rev. A **61**, 063801 (2000).
52. V. S. Yakovlev, M. Ivanov, and F. Krausz, "Enhanced phase-matching for generation of soft X-ray harmonics and attosecond pulses in atomic gases," Opt. Express **15**, 15351–15364 (2007).
53. M. B. Gaarde, J. L. Tate, and K. J. Schafer, "Macroscopic aspects of attosecond pulse generation," J. Phys. B **41**, 132001 (2008).
54. C. Jin, A. T. Le, and C. D. Lin, "Medium propagation effects in high-order harmonic generation of Ar and $N_2$," Phys. Rev. A **83**, 023411 (2011).
55. C. Jin, G. Wang, A. T. Le, and C. D. Lin, "Route to optimal generation of soft X-ray high harmonics with synthesized two-color laser pulses," Sci. Rep. **4**, 7067 (2014).
56. C. T. Chantler, K. Olsen, R. A. Dragoset, J. Chang, A. R. Kishore, S. A. Kotochigova, and D. S. Zucker, "X-ray form factor, attenuation and scattering tables (version 2.1)," National Institute of Standards and Technology, 2005, http://physics.nist.gov/ffast.
57. C. M. Heyl, J. Güdde, A. L'Huillier, and U. Höfer, "High-order harmonic generation with μJ laser pulses at high repetition rates," J. Phys. B **45**, 074020 (2012).
58. J. Rothhardt, M. Krebs, S. Hädrich, S. Demmler, J. Limpert, and A. Tünnermann, "Absorption-limited and phase-matched high harmonic generation in the tight focusing regime," New J. Phys. **16**, 033022 (2014).
59. C. M. Heyl, H. Coudert-Alteirac, M. Miranda, M. Louisy, K. Kovacs, V. Tosa, E. Balogh, K. Varjú, A. L'Huillier, A. Couairon, and C. L. Arnold, "Scale-invariant nonlinear optics in gases," Optica **3**, 75–81 (2016).
60. C. M. Heyl, C. L. Arnold, A. Couairon, and A. L'Huillier, "Introduction to macroscopic power scaling principles for high-order harmonic generation," J. Phys. B **50**, 013001 (2017).
61. P. Ye, H. Teng, X.-K. He, S.-Y. Zhong, L.-F. Wang, M.-J. Zhan, W. Zhang, C.-X. Yun, and Z.-Y. Wei, "Minimizing the angular divergence of high-order harmonics by truncating the truncated Bessel beam," Phys. Rev. A **90**, 063808 (2014).
62. A. Dubrouil, O. Hort, F. Catoire, D. Descamps, S. Petit, E. Mével, V. V. Strelkov, and E. Constant, "Spatio-spectral structures in high-order harmonic beams generated with terawatt 10-fs pulses," Nat. Commun. **5**, 4637 (2014).
63. H.-W. Sun, P.-C. Huang, Y.-H. Tzeng, R.-T. Huang, C. D. Lin, C. Jin, and M.-C. Chen, "Extended phase matching of high harmonic generation by plasma-induced defocusing," Optica **4**, 976–981 (2017).
64. H.-S. Chan, Z.-M. Hsieh, W.-H. Liang, A. H. Kung, C.-K. Lee, C.-J. Lai, R.-P. Pan, and L.-H. Peng, "Synthesis and measurement of ultrafast waveforms from five discrete optical harmonics," Science **331**, 1165–1168 (2011).